NMR introscopy

V. A. Atsarkin, G. V. Skrotskiĭ, L. M. Soroko, and É. I. Fedin

Institute of Radiotechnology and Electronics of the Academy of Sciences of the USSR,
Moscow Physicotechnical Institute, Dolgoprudnyĭ (Moscow Oblast'),
Joint Institute of Nuclear Research, Dubna (Moscow Oblast'),
and Institute of Elementoorganic Compounds of the Academy of Sciences of the USSR
Usp. Fiz. Nauk **135**, 285–315 (October 1981)

This review presents the physical foundations of NMR introscopy, a method of obtaining images by nuclear magnetic resonance. We describe various methods of producing NMR images and compare their characteristics. We discuss the technical, instrumentation, and applied aspects of NMR introscopy, and in particular the prospects for applying it in biology and medicine.

PACS numbers: 42.30.Va

CONTENTS

1. INTRODUCTION

The ensemble of methods that enable one to reveal the inner structure of opaque objects without destroying them is the object of introscopy (inner vision). The vast cognitive and applied significance of introscopy is evident. Its various methods, which employ X-rays, γ-rays, neutrons, fast ions, ultrasound, etc., are widely applied in the most varied fields, from the defectoscopy of industrial products to medical diagnostics.

Along with the development and perfection of the traditional methods, among which x-ray reconstructive tomography[1] has met with special success, in recent years a new field has arisen: NMR introscopy, which rests on the well developed technology of nuclear magnetic resonance (NMR).

As we know, nuclear magnetic resonance has been employed successfully for a long time for studying the inner structure and dynamics of matter on the atomic-molecular level (see, e.g., Refs. 2–4). Here the specimen to be studied is placed in a homogeneous magnetic field. The information obtained, which consists of the NMR spectra and the nuclear spin relaxation times, pertains to the entire volume of the specimen as a whole, without revealing its spatial macroscopic structure.

On the contrary, NMR introscopy is based on singling out the NMR signals from individual volume elements of the object of study. For this purpose one places the latter in a deliberately inhomogeneous magnetic field. After appropriate processing, the spectra of these signals enable one to obtain information on the distribution of nuclear magnetic moments and on their dynamic characteristics throughout the volume of the specimen. This idea was first realized by Lauterbur[5] in 1973, and several more effective methods for its technical realization[6–8] were soon proposed.[1)]

The path traveled by NMR introscopy during these several years looks impressive, even against the background of the present-day headlong development of science and technology. While the cited pioneer studies of the early seventies had the aim of NMR imaging of very simply model objects, at present this method is used to obtain detailed pictures of cross-sections of tissues and organs of animals and man *in vivo*, thus recognizing various pathological changes, and in particular, malignant tumors (Sec. 4c). Naturally, all this draws close attention to the new method from both its potential users—physicians and biologists—and from the inventors and developers—physicists and radio engineers. This review is mainly addressed to the latter of these categories of specialists. Its major aim is to present as clearly as possible the physical principles and technical methods on which the best known and most promising methods of NMR introscopy are based. The

[1)] Similar ideas had been advanced even earlier; see, e.g., Ref. 89.

 0038-5670/81/100841-19$01.10

biological and medical aspects will be touched upon only on the illustrative level, while the examples presented of NMR images are designed mainly for comparison of the sensitivity, information content, and resolving power of the different methods.

We assume that the reader is acquainted (if only in most general outline) with the physical foundations and technology of NMR. Nevertheless, Sec. 2 a of this review briefly presents these topics in the minimum space needed for introducing the fundamental concepts and notation that we shall use later on. We refer those wishing to acquaint themselves with this material in greater detail to the monographs of Refs. 2–4.

This review has been based on the studies published up to September 1980.

2. PHYSICAL FOUNDATIONS OF NMR INTROSCOPY

a) General information on nuclear magnetic resonance

The phenomenon of NMR amounts to the selective interaction of the nuclear magnetic moments of matter with a radiofrequency (rf) field at a definite (resonance) frequency. In order to observe NMR, one places the specimen to be studied, which contains nuclei having a spin $I \neq 0$ (e.g., ^{1}H or ^{19}F), in a strong enough dc magnetic field having the induction $\mathbf{B}_0$. The quantization of the spin moment gives rise to $2I+1$ magnetic sublevels that differ in orientation of the nuclear spin and in the associated nuclear magnetic moment μ_1 in the field $\mathbf{B}_0$. In the simplest case of $I=1/2$, there are only two such sublevels, and here the energy spacing between them is

$$\Delta\mathscr{E} = 2\mu_1 B_0 = \hbar\gamma B_0.$$

Here $\gamma = \mu_1/\hbar I$ is the nuclear gyromagnetic ratio.

The interaction of the nuclear spins with the other degrees of freedom (thermal motion of the molecules in a liquid, crystal-lattice vibrations in solids) gives rise to longitudinal magnetic relaxation with the characteristic time τ_1. This establishes thermodynamic relaxation: the preferential occupation of the lower magnetic sublevel and the appearance of a macroscopic nuclear magnetization $\mathbf{M}$ directed along the field $\mathbf{B}_0$.

Transitions between the nuclear magnetic sublevels can be excited by a rotating, circularly polarized magnetic field ($B_1 \cos\omega t$, $-B_1 \sin\omega t$) or by an ac magnetic field $2B_1 \cos\omega t$ linearly polarized in a plane perpendicular to $\mathbf{B}_0$ that has the frequency ω and satisfies the resonance condition

$$\omega = \gamma B_0 \equiv \omega_0. \tag{1}$$

This same phenomenon can also be described in classical language. In the field $\mathbf{B}_0$ the nuclear magnetic moments undergo Larmor precession around the direction of $\mathbf{B}_0$. The frequency of this precession is defined by the condition (1). A linearly polarized field can be resolved into two circularly polarized fields rotating in opposite directions. The component of the circularly polarized ac field that rotates synchronously with the nuclear moment interacts effectively with it and consequently alters its orientation. The other component does not give rise to transitions at the frequency ω. The classical description of magnetic resonance is exact enough in many cases, and hence the graphic picture of precessing magnetic moments often proves very useful.

For the usually employed fields $B_0 \sim 1$T, the frequency $\nu_0 \equiv \omega_0/2\pi$ lies in the meter range of radio waves (protons have $\gamma/2\pi = 42.57$ MHz/T). Thus the experimental technique of NMR belongs to the field of radiospectroscopy. The energy of the quanta in the radio range is considerably smaller than the energy of thermal motion of the atoms, and all the smaller in comparison with the energy of a chemical bond. Therefore the study of the inner structure of matter by NMR methods causes no physical and chemical changes in specimens. Thus the NMR methods are nondestructive testing methods.

One can observe the NMR signals in two fundamentally different ways. In the first of these, which is called the stationary method, the specimen is irradiated with a very weak rf field at the constant frequency ω, while the field B_0 is slowly varied so as to pass through resonance (or conversely, the field B_0 is kept constant, while the frequency ω is slowly varied). In a state of thermal equilibrium, the lower magnetic sublevel is somewhat more populated than the upper level, while the probabilities of transitions between the magnetic sublevels ($1 \rightleftarrows 2$) stimulated by the rf field are the same. Therefore the interaction of the nuclei with the resonance field leads to absorption of energy from the latter; this is detected by using ordinary radiotechnical methods. The outcome of such an experiment is the NMR spectrum—the relationship of the absorption coefficient χ'' to the field B_0, or equivalently, to the frequency ω. The sensitivity of this method is small, while it takes a rather long time to record the spectrum.

The other method, termed the pulsed method, consists in subjecting the specimen to a short and sufficiently intense pulse of an rf field at the resonance frequency with the duration $t_p = \pi/2\gamma B_1$. Such a pulse synchronously rotates by 90° all the nuclear magnetic moments, which were initially oriented along the direction $\mathbf{B}_0 \parallel z$. Immediately after such a "$\pi/2$-pulse" ceases, Larmor precession of the macroscopic nuclear magnetization $\mathbf{M}$ in the xy plane occurs—the so-called free induction (FI). It is detected by the emf induced in an appropriately oriented receiver coil.

With the passage of time, the precession of the individual nuclear magnetic moments becomes dephased owing to spin-spin interactions. This leads to a free-induction decay (FID) having the characteristic transverse spin relaxation time τ_2. The decay of the FI signal also arises from the scatter in the resonance frequencies of the individual nuclear spins, which is associated with the spatial inhomogeneity of the field $\mathbf{B}_0$. However, in this case the decay of the FI signal is not irreversible, and the nuclear magnetic moments can be again phased by employing additional rf pulses. As a result a "spin echo" signal arises that reproduces the shape of the FID.

The observed FI signal amounts to a superposition of the free-induction signals from all the nuclear spins of the specimen. Thus it contains full information on the frequency NMR spectrum, to which it is related by Fourier transformation. Instruments that employ this method for obtaining spectra and are equipped with a computer for Fourier transformation are called Fourier NMR spectrometers. While more complex and expensive than the spectrometers for observing stationary NMR signals, they enable a considerably higher sensitivity to be achieved, which is equivalent to shortening the time for obtaining the spectra.[9]

The information that one can obtain by using NMR is very extensive. The area under the contour of an NMR absorption line and the initial amplitude of the FI signal are proportional to the concentration of nuclei of the given type. Further, the natural line width δ, which is related to the relaxation time by $\delta \sim 1/\tau_2$, is highly sensitive to the state of aggregation of the material and to the molecular mobility. In solids the magnitude of δ is usually determined by the magnetic dipole interaction between the nuclei, and attains values of the order of 10^4 Hz. In liquids, where the dipole interactions are averaged out by the rapid motion of the molecules, the width of the NMR line declines sharply, and usually amounts to from 100 to 1 Hz. In this case one can resolve the fine structure of the spectrum that arises from the interaction of the nuclear spins with the electron cloud of the atom or molecule (the so-called chemical shifts of the NMR frequency), and also from the scalar component of the nuclear-nuclear interaction that does not vanish upon motion. High-resolution NMR spectra have the greatest information content: they enable one to decide on the subtle details of the chemical bonding and structure of molecules.[10]

The longitudinal spin relaxation time τ_1, which depends strongly on the degree of molecular mobility and is especially sensitive to the presence of paramagnetic ions and free radicals, also conveys substantial information.

b) The principle of NMR introscopy

The procedure of NMR introscopy amounts to the construction on a recording instrument (on an oscillograph or chart recorder, or in the memory of a computer) of a so-called NMR image. The status of each of its elements, e.g., the brightness and color at the given point on an oscilloscope screen, is determined by the amplitude of the NMR signal from the corresponding volume element of the object of study. This amplitude is proportional to the number of resonating nuclei. Hence the image thus obtained primarily characterizes the spatial distribution of the nuclear spins—the so-called spin density $\rho(x,y,z)$. Moreover, with an appropriate methodology, the observations of the NMR signals provide information also on the nuclear relaxation times. As we have noted above, the latter depend very highly on the state of aggregation and the chemical composition of the material being studied. This situation is very valuable, since it enables one to produce in an NMR image contrast between materials, tissues, and organs that differ only slightly in composition.

Thus the study of the spatial distribution of NMR signals makes it possible to compose a picture of the state of aggregation and chemical structure of an object inhomogeneous in composition, i.e., to solve fully the fundamental problem of introscopy.

In order to obtain NMR images, one must distinguish the NMR signals that arrive at the receiving system from different parts of the specimen, i.e., label them by using some parameter that depends on the coordinates. One can take as such a label the frequency ω_0 of nuclear magnetic resonance. If one makes the magnetic field B_0 spatially inhomogeneous, i.e., dependent on the coordinates: $B_0 \equiv B_0(x,y,z)$, then the NMR frequency, which is proportional to the coordinates, will be related to the coordinates:

$$\omega_0 \equiv \omega_0(x, y, z) = \gamma B_0(x, y, z).$$

According to this relationship, each value of the frequency of the resonance signal can be correlated with the volume element from which it was obtained. This is the general principle of most of the methods of obtaining NMR images.

In principle the resolving power of these methods is restricted only by the degree of inhomogeneity of the field B_0 attainable in practice and by the natural width δ of the NMR line. Thus, the resolution Δx along the x axis is determined by the relationship

$$\Delta x \approx \frac{\delta}{\gamma G_x}. \qquad (2)$$

Here G_x is the gradient of the field B_0 in the x direction (as always in NMR, we assume the field B_0 to be unidirectional. That is, it is characterized by a single component B_{0z}, so that, e.g., $G_x = \partial B_{0z}/\partial x$, etc.). We see from (2) that one can attain a better resolution only when the line width is small, i.e., in liquid media. Therefore one deals in NMR introscopy preferentially with liquid or "semiliquid" objects. In studying biological structures, one is mainly concerned with the spatial distribution of the physiological liquids, i.e., ultimately with water, in the organ or organism under study. The prospects of NMR introscopy of solids have as yet only been hinted at (see Sec. 3 h).

Upon adopting for example the values $G_x = 0.1$ T/m, $\gamma/2\pi = 42.6$ MHz/T (^{1}H nucleus), and $\delta = 1$ Hz, we obtain from (2) the value $\Delta x \approx 0.2$ μm. This satisfies the strictest requirements on image quality. Anticipating later discussion, we not that this resolution has not yet been reached in practice, though the reasons for this are more of technical than fundamental nature.

We must stress that, in contrast to optics, the spatial resolution of the NMR-introscopic methods is in no way limited by the wavelength of the rf field employed ($\lambda = 1$–10 m). Of course, there is no violation of the uncertainty principle here. The point is that the spatial selection (singling out of the volume element) is performed in this case by employing two fields at the same time: a dc field B_0 and an rf field $2B_1 \cos \omega t$, which are spatially coupled by means of resonating nuclear magnetic moments. This characteristic fea-

ture of the method is reflected in the name that Lauterbur[5] proposed for it of "zeugmatography" (from the Greek ζευγμα, that which binds), which has become rather widespread in the scientific literature.

If it were possible to assign a configuration of the static field $B_0(x,y,z)$ to make its value differ at each of the points of the volume under study, then a mutually single-valued correspondence between the Larmor frequency ω_0 and the coordinates x, y, and z would arise. Then the obtaining of NMR images would constitute no special problem. However, the Maxwell equations do not allow such a structure of the magnetic field. For any configuration of $B_0(x,y,z)$, two-dimensional surfaces exist on which the value of B_0 (and hence also of ω_0) does not vary. The nuclear spins lying in a thin layer of the specimen adjoining such an "isochromatic" surface unavoidably contribute to the same NMR signal. That is, they prove indistinguishable. In this regard, the construction of the final picture of the distribution of nuclear spins throughout the volume faces difficulties. The various methods of surmounting them constitute the essence of the many methods that have been developed up to now. We shall examine the most widespread and promising of them thoroughly in the next section.

3. METHODS OF PRODUCING NMR IMAGES

a) Reconstruction from projections

The first method of obtaining NMR images was proposed by Lauterbur in his pioneer study.[5] In this method one superimposes on the spatially homogeneous component of the magnetic field $B_{00}=\text{const}$ a constant grandient $G_x=\text{const}\neq 0$, $G_y=G_z=0$. Thus the resultant field increases linearly in the direction of the x axis, while the condition for NMR at the frequency of the rf field has the form

$$\omega = \omega_0(x') \equiv \gamma(B_{00}+G_x x').$$

Evidently this condition is satisfied only in a plane layer of thickness Δx perpendicular to the x axis (Fig. 1).

The NMR signal at the fixed frequency ω arises from the volume elements lying in the given layer, while the dependence of the amplitude of this signal on ω (or on B_{00}), i.e., the NMR spectrum, defines the one-dimensional projection of the function $\rho(x,y,z)$ on the x direction.

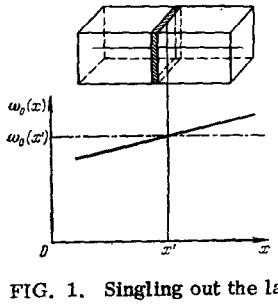

FIG. 1. Singling out the layer (hatched) that gives an NMR signal at the frequency ω in the presence of the magnetic-field gradient G_x. Below—NMR frequency distribution along the x axis.

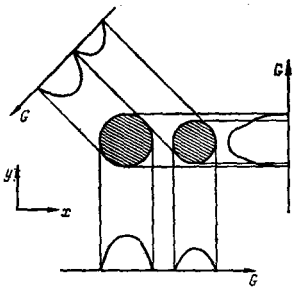

FIG. 2. One-dimensional projections of the spin-density distribution from a specimen in the form of two homogeneous cylinders oriented along the z axis for different directions of the gradient of the magnetic field G.

In order to obtain information on the distribution of nuclei in the xy plane, one repeats this experiment many times, while rotating the direction of the field gradient or the specimen each time around the z axis by some angle. This procedure is illustrated in Fig. 2 with the example of three projections for the case in which the "specimen" consists of two parallel cylinders of differing diameters.

One can construct the two-dimensional projection of the object on the xy plane from the set of one-dimensional projections thus obtained by employing a special computer program. The methods of solving this type of problems are well known and are employed, in particular, in reconstructive x-ray tomography.[1,11] We note that the very principle of reconstructing an object from its projections seems very natural: in essence we act in this very way when we turn in our hands a transparent object of interest to us and examine it from different sides.

In the example given in Fig. 2, the construction of the two-dimensional projection exhausts the problem, since for specimens homogeneous along the z axis, all cross-sections perpendicular to this axis are equivalent. Yet if cylindrical symmetry is lacking, one must extend the experiment by rotating the direction of the gradient gradually about a different axis. However, in practice, one more often proceeds in a different way. One singles out a thin "working" layer in the specimen perpendicular to the z axis, and constructs its two-dimensional NMR image, or tomogram, without displacing the gradient of the field B_0 outside the plane of this layer. Then one repeats the entire cycle of measurements in other layers to obtain a stack of tomograms, which constitutes the full volume image of the object.

The thin layer is singled out by using a special (plane) shape of the rf coils of the NMR spectrometer or by one of the selective methods described below in Secs. 3 d, e.

In a discrete (numerical) processing of the data, one constructs the image from a finite number of elements (cells), each of which corresponds to an element of the volume being studied (Fig. 3). If the number of "steps" along each of the orthogonal directions is n, the two-

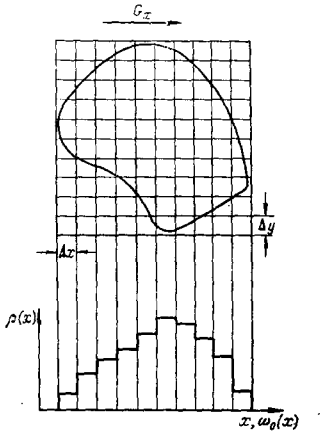

FIG. 3. Dissection of a two-dimensional object into elements (above) and the one-dimensional projection of the spin density $\rho(x)$ for discrete processing of the data.

dimensional image contains n^2, and the three-dimensional image n^3 such elements. Evidently, in order to fill all these cells, one must have the same number of equations relating the unknown values of the spin density in each of the elements to the observed amplitudes of the NMR signals. Evidently, each one-dimensional projection yields only n such equations, since the projections of the volume elements that lie in the same column are superposed on one another (Fig. 3). Thus an unambiguous construction of a two-dimensional pattern requires n independent measurements (projections), while a three-dimensional pattern requires n^2. Hence we see that, to obtain an image with a spatial resolution of the order of 1 μm, a specimen of size about 10 cm must be divided into $n \sim 10^5$ layers. In this case the number of projections reaches an astronomical value, while the information thus obtained cannot be handled on any contemporary computer. Accordingly, in practice the number of projections does not exceed 100–200. As we have said, here one usually restricts the treatment to two-dimensional images (tomograms). The number of image elements can also be larger than the number of original data. In this case one employs special algorithms that solve the problem of underdetermination. Of course, this involves losses in the resolving power of the method.

It is instructive to examine the result of Lauterbur's first experiment performed in 1973 (Fig. 4).[5] This shows a transverse section of two test tubes containing water, 1 mm in diameter and lying 3 mm apart. The image was obtained by using only four projections (the direction of the gradient of B_0 was rotated by 90°) at $\nu = 60$ MHz and $|\operatorname{grad} B_0| \approx 0.02$ T/m. The number of image elements is 20×20, and the attained resolution was about 0.2 mm.

In order to demonstrate the analytical potentialities of the method, the two test tubes were immersed in a vessel containing heavy water (D_2O). As we should expect, the deuterium nuclei, which have a different gyromagnetic ratio from the protons, gave no contribution to the observed pattern.

FIG. 4. NMR image of a cross-section of two parallel capillaries containing water.[5]

This same first experiment showed the possibility of selection in terms of nuclear relaxation times. In order to do this, one of the test tubes was filled with a dilute solution of a manganese salt instead of water. As we know, this greatly shortens the spin-lattice relaxation time of the hydrogen nuclei. When the amplitude of the resonance rf field was large enough, the NMR signal from the protons of the pure water was saturated, and only the image of the test tube containing the salt solution remained in the picture. Thus a contrast in the NMR image was observed here that arose from the difference in chemical composition.

In the experiment of Ref. 5, the NMR spectra corresponding to the one-dimensional projections of the spin density were recorded by the stationary method. As we have already noted, this possesses a low sensitivity and requires large expenditures of time to obtain an image. One can substantially improve the situation by employing FID signals that arise after $\pi/2$-pulses (Sec. 2 a). Just as in continuous recording, Fourier analysis of this signal yields a one-dimensional projection of the spin density onto the defined direction. In this case all this information is obtained from a single FID signal that decays in the time necessary for dephasing of the precession of the nuclear magnetic moments of the whole specimen in the inhomogeneous magnetic field:

$$t \approx \frac{1}{\gamma G_x L_x}.$$

Here L_x is the linear dimension of the specimen in the x direction. Since this dephasing is reversible, the FID signals can be repeated many times by the spin echo method so as to accumulate the information during the irreversible transverse relaxation time τ_2. Consequently one obtains a gain in sensitivity of about a factor of $\sqrt{n}$.

Examples of images obtained by the method of reconstruction from sections are given in Refs. 13–16. One of them is shown in Fig. 5.[15] This shows a cross-section of the test object, which was made from a Teflon washer having an N-shaped hole. The washer was placed in an ampoule containing water. The plane of the image is fixed by the height of the receiving coil. The dimensions of the washer and its orientation in the gap of the magnet are shown in Fig. 5a. The forms of

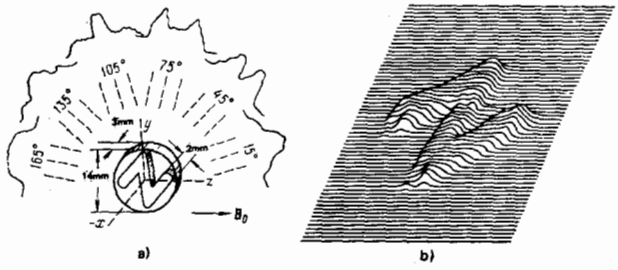

FIG. 5. Obtaining of the NMR image of a test object in the form of a Teflon disk having an N-shape hole filled with water.[15] a) The object and its one-dimensional projections; b) the NMR image obtained by reconstruction from projections.

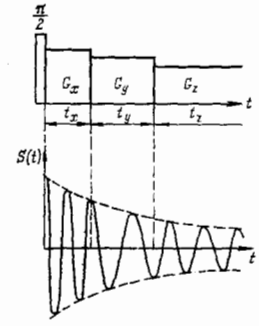

FIG. 6. Switching sequence of the mutually orthogonal magnetic field gradients G_x, G_y, and G_z (above) and the observed free-induction decay signal $S(t)$ (below) in the method of Fourier introscopy.[18]

the spectra corresponding to different orientations of the gradient of B_0 are shown in the upper part of the diagram in 30° steps. Actually the gradient was rotated in 1° steps, and the image was constructed from 180 projections. The gradient amounted to 40 μT/cm, and the NMR frequency was 8.13 MHz. After processing on a minicomputer, the resulting image was drawn on an xy plotter. This made it possible to obtain an axonometric projection of the test object (see Fig. 5b). We see that a high definition of imaging was obtained with a spatial resolution of about 0.3 mm.

Recently considerable progress has been attained in speed and resolving power of the method. Thus, the first true three-dimensional NMR images of biological objects have been recently described. They contained 33×33×33 elements and were obtained in only 7 min.[17]

b) Fourier introscopy

While the methods of Fourier spectroscopy were employed in the example given above only to improve the sensitivity, in the "Fourier zeugmatography" developed by Kumar, Welti, and Ernst[18] they are employed for reasons of principle. The method was developed to eliminate the inconvenience and loss of time involved in the multiple rotations of the specimen (or of the field gradient) in obtaining the projections according to the method of Ref. 5. The authors[18] proposed restricting the procedure to only three successive orientations of the gradient of B_0 (along the x, y, and z axes). Here all three switchings of these directions must be performed in the course of a single decay of the free-induction signal following a $\pi/2$ pulse.

The sequence of operations in this method is shown in Fig. 6. Immediately after cessation of the $\pi/2$ pulse (at the instant $t=0$), the magnetic-field gradient G_x is applied to the specimen. After the time t_x this is suddenly replaced by G_y, and after the further time t_y by G_z. The free-induction signal is observed under these conditions as a function of the time t_z. The nuclear spins lying in the volume element $\Delta x\Delta y\Delta z$ having the coordinates xyz precess about the direction of $\mathbf{B}_0$ successively with the angular velocities $\omega_0+\gamma G_x x$, $\omega_0+\gamma G_y y$, and $\omega_0+\gamma G_z z$. Hence the envelope of the FID signal from the entire specimen at the instant of time $t=t_x+t_y+t_z$ has the form

$$S(t)=\iiint \mathrm{d}x\,\mathrm{d}y\,\mathrm{d}z\,\rho(x,y,z)\exp\{i(\gamma G_x x t_x+\gamma G_y y t_y+\gamma G_z z t_z)\}. \quad (3)$$

(We shall neglect relaxation in order to simplify the presentation.)

The expression (3) amounts to a three-dimensional Fourier image of the spin density treated as a function of the Larmor frequencies $\omega_x=\gamma G_x x$, $\omega_y=\gamma G_y y$, and $\omega_z=\gamma G_z z$, which are related unambiguously to the coordinates. In an experiment one measures the FID signals as a function of t_z (with $t_x, t_y=\text{const}$), and then repeats the measurements many times, while successively varying t_x and t_y. The set of values of the function $S(t)$ thus obtained is subjected to three-dimensional Fourier transformation, and one finds the function $\rho(x,y,z)$, i.e., the NMR image of the studied object.

Analysis shows that one must take $2n$ steps for each of the intervals t_x, t_y, and t_z to obtain a picture made of $n\times n\times n$ elements.[18] The total amount of information to be stored in memory is too large in this case. Hence, just as in the Lauterbur method, in practice one usually restricts the treatment to two-dimensional images. In particular, in the study[18] cited above, an image of a cross-section of two test tubes containing water consisting of 64×64 elements was constructed. The field gradients employed in this experiment were about 2×10^{-3} T/m, while the time spent on the entire experiment amounted to 15 min, of which the printer at the output of the computer took 7 min.

In addition to the decreased number of orientations of the gradient of B_0 that we have already noted, a convenience of this method consists in the fact that a sequence of Fourier transformations is performed here instead of the complex algorithm for reconstruction from projections.[11] These transformations are widely applied in NMR technique, and are automatically realized in the modern commercial spectrometers.[19]

On the other hand, the fast switching of the magnetic-field gradients can give rise to induction currents, which are undesirable in biomedical applications.

c) Selective methods; magnetic focusing

The two methods described above (reconstruction from projections and Fourier introscopy) belong to the

class of integral methods in terms of the structure of the recorded information. The NMR signals directly recorded in the course of the measurements contain information simultaneously on many (or even on all) volume elements of the specimen, while the information on each of them individually becomes accessible only after complicated mathematical processing of the results. The advantage of the integral methods consists in their higher sensitivity, which is attained by collecting the signals from the whole specimen. At the same time, these methods involve a complicated analysis of the primary information and are highly sensitive to variation in the gradients of B_0 in space and time, and also to phase shifts and instability in the circuits of the NMR spectrometer.

These difficulties do not arise in another approach to constructing NMR images, which we can call the selective approach. In these methods the signal applied to the receiving device is collected from only one volume element, whose location is then shifted throughout the specimen according to an established rule. The image is constructed point by point and line by line, just as is done in forming a television image.

The methods of singling out (selecting) small volume elements, which we shall term below the "working" volume elements, can differ: from the somewhat straightforward, but not at all simple to execute technically, idea of magnetic focusing,[8] which will be treated in this section, to the more refined methods, including periodic modulation or pulsed switching of the field gradients (Secs. 3 d, e).

As we see from its name, the principle of magnetic focusing consists in concentrating a dc and/or a resonance high-frequency magnetic fields within the bounds of the volume element being examined. The simplest scheme of this type leaves the field B_0 homogeneous, whereas the configuration of the rf field, which is fixed by the geometry of the corresponding coils of the NMR transducer, enables one to irradiate selectively only a small fraction of the object of study. Thus, upon placing the patient in the field B_0, one applies to different parts of his body a miniature rf coil, similarly to what a physician does in listening to a patient with a stethoscope.

The greatest advances in realizing this method have been attained in the laboratory of Professor Béné (Switzerland).[20,21] Here the magnetic field of the Earth was employed as B_0. Then the NMR frequency of protons is very low—only about 2 kHz. Therefore an acceptable signal-to-noise ratio of the order of 100 is reached only with working volumes of the order of a cubic decimeter. The resolving power of this method is so low that here one can hardly speak seriously of NMR images of biological objects. Nevertheless, by employing the appreciable differences in nuclear spin relaxation times in different human organs, Béné and his colleagues have been able reliably to distinguish the NMR signals from the blood filling the heart, from the stomach contents, from the urinary bladder, etc.

We note that the observation of NMR signals from spatially localized regions in the Earth's magnetic field can prove to be of interest also as applied to extended objects of nonbiological nature, e.g., in probing mineral resources.

R. Damadian and his associates (USA) have made decisive advances in the methods of magnetic focusing. They employed a special configuration of both a dc and a high-frequency magnetic field to single out a restricted region in the object being studied.[8,22-24] As we have mentioned above, the topological characteristics of a dc magnetic field do not allow one to localize it within a restricted region of space. Nevertheless, one can create a configuration of the magnetic field B_0 in which it will be considerably more homogeneous in a relatively small volume than in the remaining regions of the specimen. The spectrum of the NMR signal from the nuclei contained in this volume will be narrower and its amplitude larger than those from the nuclei lying in adjacent regions. If, moreover, one takes care with the special construction of the rf coil, which also enables a certain concentration of the rf field in a defined region, one can attain the desired spatial selection of the NMR signal with a resolution of the order of 1 mm.[8] By this method, Damadian and his associates obtained in 1976 the image of a cross-section of a living mouse that reliably distinguished the contours of the heart and lungs.[8] The cover of the issue of *Science* in which his article was published showed the first NMR image of a malignant tumor implanted in a living mouse. Here the contrast arises from the fact that the nuclear spin-lattice relaxation time in the tissues affected by the malignant tumor is considerably larger than in healthy tissues.[25] The NMR images of cross-sections of a living person at the level of the chest, which have also appeared on the covers of scientific journals,[22-24] are even more impressive. The experiments were performed in a magnetic field of about 0.1 T (the diameter of the solenoid was 1.35 m). Here the construction of the whole image with a resolution of about 6 mm took from 4.5 hours in the first experiments[22] to 35 min in the following experiments.[24]

An evident advantage of the method of magnetic focusing is the possibility of selectively studying any part of the studied object, e.g., an organ under suspicion. The fundamental defect of the method is the relatively low sensitivity and the complexity of focusing the magnetic field. The latter difficulty even more heightens the need for scanning the defined small volume (the "resonance aperture" in the terminology of the authors of the method) throughout the object of study. This problem is solved only by using a complicated design of the magnet that was developed with a computer. The basis of this magnetic system is a gigantic superconductive solenoid.[26,27]

d) The method of the sensitive point (line)

Another example of selective NMR introscopy is the method of the sensitive point, which was proposed by Hinshaw in 1974,[7] and then perfected and reduced to biomedical applications in the laboratory of E.R. Andrew at Nottingham University.[28-41] The essence of the method

is that the entire specimen apart from one small volume element (the "sensitive point") is subjected to an audiofrequency ac magnetic field. Under these conditions one synchronously detects the NMR signal at the frequency ω_0 corresponding to the value of B_0 at the sensitive point. Evidently the dc component of the output signal contains only the contribution from the nuclei lying in the region of the sensitive point, since the NMR spectrum from the rest of the specimen proves to be modulated in frequency.

This method is realized in practice by employing three time-variant magnetic-field gradients whose directions are mutually orthogonal, while their magnitudes oscillate at different frequencies. In order to understand what happens here, let us first examine one such gradient (e.g., along the x axis), which has the form

$$G_x(t) = G_x \sin \Omega_1 t.$$

In this case the magnetic field in the specimen varies according to the law

$$B_0(x, t) = B_{00} + (x - x_0) G_x \sin \Omega_1 t.$$

We see from this relationship that the field $B_0(x,t)$ depends on the time for all x except $x = x_0$ (Fig. 7a). Those nuclei of the specimen will contribute to the observed NMR signal that lie in a layer of thickness Δx near the plane perpendicular to the x axis passing through x_0.

In practice one often generates the oscillating gradient with a pair of coaxial coils (of the Helmholtz type) supplied with alternating current, and with opposed magnetic fields. If the currents in the coils are the same, the working plane lies exactly in the middle between them. By increasing the amplitude of the alternating current in one of the coils, one can shift this plane throughout the specimen (Fig. 7b).

Analogously, a gradient $G_y(t)$ oscillating with a frequency $\Omega_2 \neq \Omega_1$ defines a plane perpendicular to the y axis. The intersection of the two working planes yields a "sensitive line," or bar of cross-section $\Delta x \Delta y$ parallel to the z axis. And finally, a gradient $G_z(t)$ oscillating with the frequency $\Omega_3 \neq \Omega_1, \Omega_2$ defines the sensitive

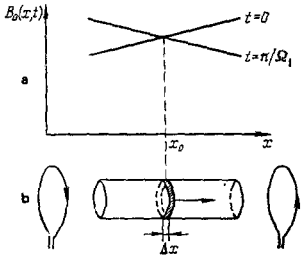

FIG. 7. Singling out the working ("sensitive") plane using a magnetic-field gradient that oscillates in time with the frequency Ω_1.[7]

a) Magnetic-field distribution along the x axis for the times $t = 0$ and $t = \pi/\Omega_1$; b) location of the working plane in the specimen (hatched) and the direction of its displacement as the current in the gradient coils is varied.

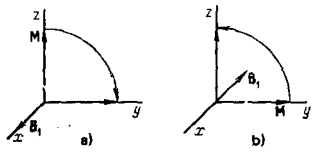

FIG. 8. Behavior of the nuclear magnetization M in the system of coordinates rotating along with the vector $\mathbf{B}_1$ in the stationary-free-induction method at the time of the first $\pi/2$ pulse (a) and of the second $\pi/2$ pulse (b).

point (x_0, y_0, z_0). Scanning of the latter allows one to construct a three-dimensional image of the entire object of study.

We note immediately that, in the contemporary variant of this method,[31-40] the third gradient, e.g., G_z is left unmodulated (static). The FI signal observed under these conditions arises from the sensitive line (x_0, y_0), along which the frequency of nuclear precession varies according to a linear law. Thus, each element of the sensitive line proves to be labeled with the frequency $\omega_0(x_0, y_0, z)$. Hence a Fourier transformation of the FI signal enables one to find directly the spin-density distribution along the line $\rho(x_0, y_0, z)$.

After this stage is completed, the sensitive line is shifted for a small distance in the plane of the cross-section being studied, the procedure is repeated, etc., until the required tomogram has been obtained.

The method of recording NMR signals adopted here is based on the so-called stationary free induction. The specimen is subjected to a sequence of $\pi/2$ pulses in which the phase of the rf field is in turn shifted by 180°. Figure 8 illustrates the behavior of the nuclear magnetization M in the system of coordinates rotating in the direction of the nuclear Larmor precession at the frequency ω_0. Before the pulses begin to act, the magnetization lies along the z axis. After the first pulse, during which the rf field $\mathbf{B}_1$ lies along the x axis, the magnetization is rotated by 90° and is oriented along y. After the second pulse, in which $\mathbf{B}_1$ is directed along $-x$, the magnetization returns back to the z axis, etc. Let the time T between the pulses be much shorter than the characteristic longitudinal and transverse spin relaxation times τ_1 and τ_2. Then the decrease in the magnetization during the time that it is perpendicular to the z axis amounts to $M\tau_2/T$, while its increase owing to longitudinal relaxation in the period when it is parallel to z is $(M_0 - M)\tau_1/T$. Here M_0 is the equilibrium magnetization. In a stationary regime these quantities are equal to one another. This implies that

$$M_{stat} = \frac{M_0}{1 + (\tau_1/\tau_2)}. \qquad (4)$$

This expression determines the amplitude of the free-induction signal measured in the sensitive-line method. We see from (4) that, when $\tau_1 \approx \tau_2$ as is characteristic of many liquids, the value of M_{stat} amounts to about $M_0/2$. That is, it is relatively large, whereas for solids, for which $\tau_1 \gg \tau_2$, the signal approaches zero. The sensitivity to nuclear relaxation times implied by (4) enables a high contrast of the images with respect

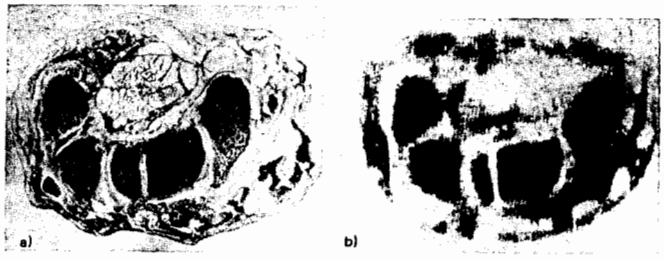

FIG. 9. NMR image of a thin cross-section of the left wrist of a person obtained *in vivo* by the sensitive-line method (the darker regions correspond to larger NMR signals) (b), and a photograph of the corresponding cross-section in a cadaver (a) (according to Refs. 35, 38).

to the state of aggregation and chemical composition of the object being studied, which renders this method very attractive.

A theoretical analysis of the resolving power[41] has shown that the effective thickness of the sensitive line along the x or y axis amounts to

$$\Delta x = \Delta y \approx \frac{3.5}{\gamma G_\xi T}. \tag{5}$$

Here $\xi = x$ or y, while the spatial resolution along the line is

$$\Delta z \approx \frac{3.8}{\gamma G_z T}. \tag{6}$$

Since $T \ll \tau_1, \tau_2$, the relationships (5) and (6) imply that stronger magnetic field gradients are required here to obtain the same resolution than in the method of reconstruction from projections [see (2)].

On the other hand, the undoubted advantages of the sensitive-line method are its relative simplicity and the less rigorous requirements on homogeneity of the values of G_x, G_y, and B_1.

The noted practical advantages have had the result that but little time has passed from the first experiments on model objects (still the time test tubes containing water) to the attainment by the sensitive-line method of high-quality images of biological objects. These images have been reproduced repeatedly in various publications,[31,33-39] including the covers of scientific and popular-scientific journals.[31,42] One of them, which amounts to the NMR tomogram of a person's wrist, is shown in Fig. 9.[2)] The experiment was performed with $\nu = 30$ MHz, $B_0 = 0.7$ T, and $|\operatorname{grad} B_0| \approx 10^{-2}$ T/m. The resolution attained was 0.4 mm, and the duration of the experiment was 9 minutes. We see in the image practically all the details of the wrist: bones, inside of which one discerns an intense signal from the fat and bone marrow (dark regions), tendons, muscles, and large blood vessels.

Even more impressive results have been obtained very recently by a refined technique that includes real-time Fourier transformation of the FI signals on a fast minicomputer.[39,40] The construction of the tomogram

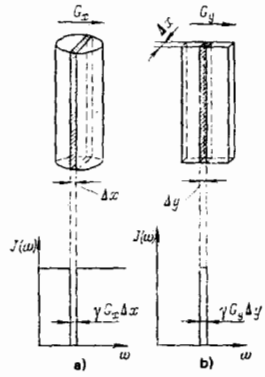

FIG. 10. Sequence of operations in the selective-excitation method.[43]
a) Singling out the working plane in the object; b) singling out the working line in the plane. Below—spectral composition of the rf $\pi/2$ pulses.

of a cross-section of the head of a person containing 128×128 elements took only 150 sec.[39] Further increase in sensitivity and speed can be obtained by combining the methods of the sensitive plane and reconstruction from projections. A corresponding example will be presented in Sec. 4c.

e) The method of selective excitation

Another method for singling out the working region has been proposed and realized by Mansfield and his associates.[43-50] In this method the stated problem is solved by a special choice of the frequency spectrum of the exciting rf pulses.

In one of the variants,[43] the specimen is placed in a magnetic field B_0 having the gradient G_x. Under these conditions it is subjected to an rf pulse whose spectrum overlaps the NMR frequencies throughout the specimen, apart from the narrow layer Δx (Fig. 10a). This pulse has an amplitude and duration that cause the resonating nuclear spins to be rotated by 90°. The precession of the nuclear magnetization that arises after the pulse has ceased decays rapidly owing to the dephasing of the motion of the individual nuclei in the inhomogeneous field. Thus, after a short time the nuclear spins of the entire specimen, except for the defined layer, drop out of play in a time of the order of τ_1. They subsequently no longer contribute to the overall signal in the receiving coil.

Then the direction of the field gradient is changed abruptly by 90°, and a $\pi/2$ pulse is again applied to the specimen. However, now its spectrum corresponds to the resonance frequencies of only the nuclei lying in the narrow layer Δy (Fig. 10b). Consequently a free-induction signal arises only from the nuclear spins that lie inside the thin bar of cross-section $\Delta x \Delta y$ parallel to the z axis. This signal is recorded after a new switchover of the field gradient, this time along the z axis, so that a Fourier transformation of the FID signal gives the spin-density distribution along the z axis in the defined volume element $\Delta x \Delta y$.

It is evident from what we have said that a successful

[2)] The authors thank Professor E. R. Andrew and Dr. P. A. Bottomley for permission to use this illustration.

realization of the Mansfield method requires careful control of the spectrum of the radiofrequency pulses. The usual square rf pulses having a constant frequency throughout the duty cycle and duration t_p prove inappropriate here. This is because, as we know, their spectrum is not only broadened by amounts of the order of $1/t_p$, but also it contains rather intense side lobes that cover a considerable frequency range. Hence in Refs. 43–50 "tailored pulses" were employed, i.e., they were formed from oscillations of different frequencies, amplitudes, and phases by using a special synthesizer controlled by a computer. This same computer, which was a part of the NMR introscope, was employed for accumulating and processing the NMR signals, for scanning the working volume element, and constructing the image.[44]

Images of biological objects of small dimensions were obtained by the described method, which was called linear scanning by its authors: hollow stems of plants, thin bones, etc.[44] The time for constructing NMR images in such a section of diameter 1.5 cm with a resolution of the order of 0.5 mm amounted to about a minute. The obtained picture was not distinguished by high quality; this apparently involved radiotechnical problems arising in the selective excitation. The point is that the correct functioning of the above-mentioned sequence of synthesized rf pulses requires very high homogeneity and phase stability of the high-frequency field, which is difficult to obtain over any significant volume. Accordingly, small specimens are apparently an inevitable feature of the given method, whose prospects should most likely be sought in NMR microscopy, i.e., in studying very small structures, e.g., cell structures.[3)] An elaboration of this method, which involves simultaneous excitation of an entire set of sensitive lines and planes, will be treated in the next section.

f) Discrete periodic structures

In all the cases treated above, the distribution of nuclear spins $\rho(x,y,z)$ was assumed continuous. Let us turn now to the situation in which the specimen under study amounts to a regular discrete structure or lattice. The interest in such objects arises from two factors: first, the distinctive nature of the process of obtaining their NMR images, and second, the practical importance and abundance of periodic and quasiperiodic structures—from crystal lattices to the cellular structure of living organisms. Moreover, as we shall see from the material below, an important role in NMR introscopy can be played by artificial periodic objects created by the method of selective excitation.

At first we shall examine, following Ref. 51, a very simple one-dimensional lattice consisting of a set of equally spaced, homogeneous plane layers of thickness Δx and period l_x, and shall assume a magnetic-field gradient G_x directed perpendicular to these planes

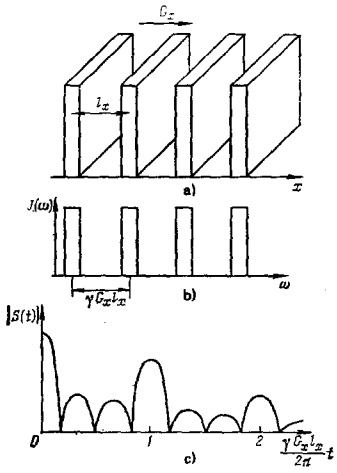

FIG. 11. "NMR diffraction" in a one-dimensional structure. a) One-dimensional grating made of parallel plane layers in the presence of a magnetic-field gradient; b) spectral composition of the free-induction (FI) signal; c) envelope of the observed FI signal.

(Fig. 11a). The free-induction signal that arises after the action of a $\pi/2$ pulse on such an object evidently contains a discrete set of frequencies separated by spacings of $\gamma G_x l_x$ (Fig. 11b). The beats between the signals from the individual plane layers produce a series of maxima on the time pattern of the FID, the principal ones of which arise at the times $t_n = 2\pi n/\gamma G_x l_x$ (Fig. 11c).

This pattern, which arises from the phase difference of the free-induction signals from adjacent planes, is fully analogous to the maxima and minima of illumination in optical diffraction by a grating, where the phase differences involve the difference in ray path from adjacent slits. The noted analogy proves to be far-reaching. It offers grounds for speaking of "NMR diffraction" and applying the mathematical apparatus developed in optics[51] in analyzing this phenomenon.

The theoretical predictions have been confirmed experimentally in the same study[51] using model objects that amount to a series of thin layers of an organic liquid separated by solid partitions about 1 mm thick. As we have noted, the NMR signals from solid specimens are strongly broadened by the dipole interactions and hence are practically invisible, whereas the intense signals from the liquid regions yield a distinct pattern of "NMR diffraction," which allows one to determine the parameters of the one-dimensional lattice. On the other hand, one can also calculate from this pattern the arrangement of the solid partitions, which are not directly detectable, and which fill the remaining fraction of the volume of the specimen (in optics this method is based on employing the Babinet principle).

In going to two- and three-dimensional lattices, the production of the images generally requires successive repetition of the experiments with different orientations of the field gradient. That is, it involves reconstruction from projections. However, the reconstruc-

[3)] In Ref. 50 a tomogram of the abdominal cavity of a person by the linear-scanning method was successfully obtained. The experiment took 40 min.

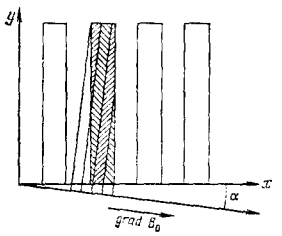

FIG. 12. On the construction of the projection of a two-dimensional periodic discrete structure on the direction of grad B_0 that forms an angle α with the x axis.

tion algorithm here can be substantially simplified as compared with Lauterbur's method.[5] Moreover, in a number of cases it turns out that a correct choice of the field-gradient direction enables one to obtain all the information from a single projection, thus shortening substantially the duration of the experiment.[45,46]

What we have said is illustrated in Fig. 12, where a two-dimensional system has been chosen as the object of study, consisting of a set of parallel strips extending along the y axis. Here the distribution of nuclear spins inside these strips is assumed to be arbitrary. We see from Fig. 12 that, if the direction of grad B_0 makes a small angle α with the x axis, then a single projection of the spin density on this direction yields information on the distribution of nuclei throughout the object, although the spatial resolution along the y axis is diminished here by a factor of $\cot\alpha$.

The method described here was the basis for development of the "planar" method of obtaining NMR images.[45-47] The singling out of the required plane and the creation in it of a periodic structure made of parallel strips are conducted here in the same way as in Ref. 43 (see Sec. 3 e). At first, one uses synthesized pulses to saturate the system of nuclear spins throughout the specimen except for one thin layer. Then, again by using specially shaped pulses, one rotates by $\pi/2$ the nuclear magnetization inside the discrete strips lying in this plane. In this case the synthesis of the rf pulses is technically even more complicated than in Refs. 43 and 44. We shall not take up this problem here, but refer the reader to Ref. 46.

We can easily convince ourselves that the described procedure for shortening the number of measurements, i.e., reducing the information on the two-dimensional object to a one-dimensional projection, can also be extended to three-dimensional periodic structures.[48] In this case all the information on the spin-density distribution along each of the parallel bars forming the regular structure can be obtained from a single projection along a direction that forms the oblique angles α, β, and γ with the x, y, and z axes. The details of the selective excitation of FID in such a structure (the method of "multiplane" NMR imaging), as well as the modification of this method using the spin-echo effect, are described in Refs. 48 and 49. All these refinements are primarily designed to shorten the time of obtaining NMR images. According to the estimates of the authors of Refs. 48 and 49, applying them should allow one to construct the image of a complete cross-section of the human body in several seconds. However, up to now it has been possible to analyze in such a time only objects of dimensions of the order of several centimeters.[43-49] This discrepancy between the theoretical estimates and practice is explained by technical difficulties mainly involving the creation in large volumes of highly uniform rf fields that are complex in composition.

g) NMR introscopy in a rotating system of coordinates

One of the defects of all the methods described above is the need of modulation or rapid switching of the magnetic-field gradients. This fact complicates the procedure of obtaining images, and can lead to induction currents in the object of study, which is especially undesirable when this object is a living organism. One of the methods of eliminating this defect has been proposed by Hoult.[52] It consists of making both magnetic fields spatially inhomogeneous: the dc field B_0 and the hf field $2B_1\cos\omega t$ perpendicular to it. That is, in addition to the gradient of the field B_0, one produces a gradient of the amplitude of the ac field B_1 perpendicular to it. Thus, if $B_0 \equiv B_{0z}$ and $G_x \equiv \partial B_{0z}/\partial x$, then one selects $B_1 \equiv (B_1)_x$, while producing the gradient $g_{y,z}$ in it along the y or z axis.

Under these conditions each volume element of the specimen proves to be labeled with two independent variables, e.g., $B_0(x)$ and $B_1(z)$. In principle, this enables one to construct a two-dimensional image of the object in the xz plane.

The method proposed[52] to realize this suggestion is explained in Fig. 13. In a system of coordinates that rotates about the direction of the z axis with the frequency ω along with the nuclear magnetization, as we know,[2] the nuclear spins sense the time-independent effective field $\mathbf{B}_e$ having the components $(B_e)_z = B_0 - (\omega/\gamma)$ and $(B_e)_x = B_1$. The magnetization vector M in this rotating system of coordinates (RSC) precesses about the direction of $\mathbf{B}_e$ with the frequency $\Omega_e = \gamma B_e$. This motion is called nutation. If $B_1 \gg |B_0 - (\omega/\gamma)|$, then we have $B_e \approx B_1$, so that when $g_z \equiv (\partial B_1/\partial z) \neq 0$, the frequency Ω_e is a single-valued function of the coordinate z, and can serve as a marker for this coordinate.

The frequency Ω_e was measured in Ref. 52 in terms of the angle φ of rotation of the nuclear magnetization during the time of action of the rf field pulse (see Fig. 13): evidently the spins, which have rotated through

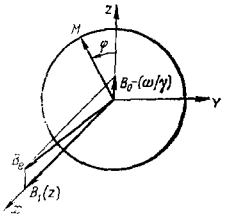

FIG. 13. Precession of the nuclear magnetization M around the direction of the effective field in the rotating system of coordinates.

different angles in the same time, give different contributions to the FI signal observed following the pulse. These measurements allow one to distinguish the NMR signals from volume elements differing in the z coordinate. As usual, the selection with respect to x is carried out in terms of the frequency of the Larmour precession in the field $B_0(x)$.

Two-dimensional projections of a set of simple objects (test tubes containing water, etc.) have been obtained by the method described in Ref. 52. A further development of this method, which has also been proposed by Hoult,[52] consists in defining the third coordinate (y in our example). For this purpose it has been proposed to employ yet another ac magnetic field parallel to the z axis. The frequency of this field is close to Ω_e, while the amplitude B_2 has a gradient along the y direction. Let us transform to the new, already doubly rotating system of coordinates (the second rotation occurs about $\mathbf{B}_e$ at the frequency Ω_e). Now we can show that the FI signals under these conditions will be marked with three independent variables: $B_0(x)$, $B_1(z)$, and $B_2(y)$. This allows us to construct the complete three-dimensional image without any switchings of magnetic fields.

h) Prospects of NMR introscopy of solid objects

As we have already noted, the strong dipole broadening of the NMR lines in solids does not allow one to apply to them directly the methods of NMR introscopy described above. Nevertheless, this problem does not seem hopeless, since recently a number of radiotechnical methods has been developed that sharply narrow the NMR lines in solid specimens. Here we shall not touch upon the essence of these methods (one can find a detailed description of them, e.g., in Ref. 53). We note only that specially chosen sequences of high-power radiofrequency pulses can decrease the width of NMR lines in solid objects by two to three orders of magnitude, so that the typical values of δ under these conditions can amount to about 10 Hz.

At first glance, it can seem that this fully exhausts the problem by liquidating the difference between NMR in solids and in liquids. However, this is actually not completely true, since the inhomogeneous width of the NMR lines is decreased simultaneously with the suppression of the nuclear dipole interactions. This partially compensates the action of the field gradient B_0 itself, which is necessary in principle for the construction of the images.

This difficulty has been overcome by Mansfield and Grannell, who have proposed a rather complicated sequence of radiofrequency pulses that suppress the dipole width of the NMR lines, while conserving the role of the magnetic-field gradient.[51] One cycle of such a sequence consists of eight coherent $\pi/2$ pulses, in which the phase of the radiofrequency field alternates in a definite way, while the direction of the gradient of B_0 is reversed in the intervals between the pulses.

By employing such a sequence of pulses, the authors of Ref. 51 obtained a satisfactory diffraction pattern from a one-dimensional grating consisting of several parallel plates made of solid camphor (see Sec. 3 f). The resolution that they attained amounted to about 0.5 mm with $|\operatorname{grad} B_0| = 7.7\times10^{-3}$ T/m.

As a maximum program, the same study[51] discusses the possible achievement of a resolution of the order of 3 Å, which would enable the employment of NMR introscopy for visualizing crystal lattices. However, the estimates show that, when $\delta \sim 10$ Hz, this would require field gradients of the order of 10^3 T/m (i.e., 100 kG/cm), which cannot be produced at present. Moreover, the narrowing of the NMR lines in solids that can be attained by the currently known methods requires certain bounds on the total variation of B_0 over the volume of the specimen: thus, in order to obtain $\delta \approx 10$ Hz, this variation should not exceed 0.1 mT. Finally, as analysis shows, a resolution of the order of several Ångström units requires the maintenance of a fantastic degree of constancy of the gradient of B_0 within the specimen. Its relative variations from point to point should not exceed 5×10^{-6} (!).[51] Thus the visualization of a crystal lattice by "NMR diffraction" as yet remains outside the bounds of real possibilities. Of course, this does not exclude applications of this technique for studying the macroscopic structure of solid objects.

Another possible approach to the problem of NMR introscopy of a solid object is based on the idea of producing an artificial narrowing of the NMR line only in a small volume element of the specimen. The latter will give the decisive contribution to the observed signal, whereas the broad and weak lines from the rest of the object will produce only an insignificant background. One of the variants has been proposed by Wind and Yannoni.[54] It is based on the so-called modulation narrowing of NMR in solids.[55] In this method a sharp decrease in δ is attained only at a definite detuning Δ between the frequency ω of the rf field, which is subjected to deep modulation, and the Larmor frequency γB_0 of the nuclei. Evidently, in the presence of a gradient G_x the condition for narrowing is satisfied only in a narrow working layer lying perpendicular to the x axis, so that the NMR spectrum gives a one-dimensional projection of the spin density, just as in the Lauterbur method[5] (see Sec. 3 a).

Here, as in Ref. 5, a set of projections is required for constructing the complete image. However, this can be avoided by using the idea of NMR introscopy in a rotating system of coordinates, as described in Sec. 3 g. When applied to solid specimens, this method must be modified; one of the possibilities consists in using the so-called "magic angle"

$$\theta_M = \arccos\frac{1}{\sqrt{3}} \tag{7}$$

between the effective field $\mathbf{B}_e$ acting in the RSC and the z axis (Fig. 14). As we know, fulfillment of the condition (7), which can be written otherwise as

$$B_0 - \frac{\omega}{\gamma} = \sqrt{2}\,B_1, \tag{8}$$

leads to a considerable decrease in the dipole width of NMR in solids.[56] In the presence of the gradients G_x

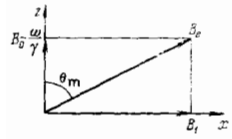

FIG. 14. The effective field in the rotating system of coordinates under the conditions of the "magic angle" θ_m between the effective field B_e and the z axis.

and g_z we have

$$B_0 \equiv B_0(x), \quad B_1 \equiv B_1(z).$$

Thus the relationship (8) is converted into an equation relating the x and z coordinates of the volume element being imaged.

Now, as is done in Ref. 57, let us observe the NMR signal that arises in the rotating system of coordinates at the frequency

$$\Omega_e = \gamma B_e(x, z) = \sqrt{[\gamma B_1(z)]^2 + [\gamma B_0(x) - \omega]^2}. \qquad (9)$$

Then the simultaneous solution of the two equations (8) and (9) unambiguously defines both of the cited coordinates. With an appropriate scanning, this enables the construction of a two-dimensional image.

As in the method of Hoult,[52] Sec. 3g, one can make the transition to a three-dimensional picture by employing resonance in a doubly rotating system of coordinates. We stress that here an even stronger narrowing of the NMR lines should occur in a solid.[58]

In practice the application of the method of Wind and Yannoni has not gone beyond the construction of a one-dimensional projection of a model object amounting to two crystals of adamantane,[54] while the variant that we have described last has not yet been realized at all. Nevertheless, the unswerving and rapid progress of the technique of NMR in solids allows us to hope for a successful solution of the problem in the very near future.

4. APPLIED AND TECHNICAL ASPECTS

a) The problem of sensitivity

The main defect, which is inherent in all methods of NMR instroscopy without exception, is their low sensitivity, which leads to a need for accumulation of signals and substantially increases the time taken by the measurements. This feature is a fundamental one and it involves the relatively low frequency of NMR as compared with other spectroscopic methods, i.e., the low quantum energy in the radio range. Therefore, when one works on refining methods of NMR introscopy, one must adopt the aim, not so much to reach the sensitivity characteristic, say, of x-ray radiography which is known to be impossible, as to enable a satisfactory signal-to-noise ratio to be achieved in a practically acceptable time.

There are two approaches to analyzing the sensitivity in constructing NMR images. The first of them, which has been most fully presented by Brunner and Ernst,[59] is of a general, purely theoretical nature. It does not take into account the instrumental aspects of the problem. From this standpoint, one should compare the various methods described above in terms of two parameters: the energy E_0 of the signal input into the receiving system per unit time, and the overall time T_0 of collecting the information. The first of these quantities is proportional to the number of volume elements $\Delta x \Delta y \Delta z$ of the specimen that simultaneously contribute to the measured NMR signal. Thus, if we assume for a specimen containing $n \times n \times n$ elements that the sensitive-point method[7] yields $E_0 = 1$ in arbitrary units, then the methods that single out a sensitive line[31,43] are characterized by the signal energy $E_0 = n$; in recording a defined plane[5,46] we have $E_0 = n^2$; and finally, in the method of reconstruction from projections by Fourier transformation of the FID signal we have $E_0 = n^3$, since here the FID signal arises simultaneously from the entire specimen.

On the other hand, the overall time T_0 of the experiment is proportional to the number of intermediate experiments. As a rule, the latter consist in measuring the FID signal for different values of the field gradients. Here the sensitive-point methods with n^3 independent measurements and the method of reconstruction from projections, for which $T_0 \propto n^2$, yield the poorest results. The record-making speed belongs to multiplane NMR introscopy,[48] in which all the information is collected while recording a single FID signal.

Since the signal-to-noise ratio is proportional to $\sqrt{E_0/T_0}$, an ideal method should combine simultaneous excitation of the entire specimen with application of time-dependent field gradients that would enable an unambiguous marking of all the volume elements. Apparently such a program has not yet been fully realized, although multiplane introscopy employing spin echo[48] approaches rather close to this goal.

The other approach yields substantially different conclusions. Here purely practical considerations stand uppermost—such as the choice of working frequency, the attainable homogeneity and stability of the magnetic fields, losses in the specimen, etc. Thus, Hoult and Lauterbur[60] have analyzed the sensitivity in constructing images of biological objects (in particular, the head, torso, and extremities of a person). They concluded that the dielectric losses can be made negligibly small with an optimal geometry of the transmitting and receiving coils. In their view, the decisive role is played by the magnetic losses, which arise from the induction currents in the conductive medium, and which govern the signal-to-noise ratio at a working frequency $\nu \geq 10$ MHz. At lower frequencies ($\nu \lesssim 1$ MHz) these losses become insignificant, although the sensitivity declines here as $\nu^{7/4}$. The numerical estimates performed in this same study[60] show, in particular, that one can obtain FID with a signal-to-noise ratio of about 50 for a volume element of 1 cm^3 filled with biological tissue (brain substance) at a frequency of 1 MHz, and of about 250 at a frequency of 4 MHz. Other authors[61,62] have arrived at similar conclusions.

Bottomley's[63] comparison of all the known practical results (up to 1979) on construction of NMR images

TABLE I. Time expenditures in constructing NMR tomograms

Method	Reference	Object	ν_0, MHz	d, cm	n^2	T, min		
						Experiment	Calc. (a)	Calc. (b)
Reconstruction from projections (continuous method of NMR recording)	12	Branch of a coniferous tree	8.13	2.8	32×32	20	67	38
Reconstruction from projections (pulsed NMR recording)	13	5 tubes containing water	30	8	32×32	0.25	50	6
Fourier introscopy	18	2 tubes containing water	—	—	64×64	8	—	—
Sensitive point	29	Stem of a green onion	60	0.8	28×28	120	1100	130
Sensitive line	31, 33	Human wrist	30	8	128×128	8	3	0.4
Linear scanning	64	Tumor on the paw of a living rat	15	1.7	64×64	13	13	12
Selective excitation of a plane using the spin echo	48	Toroid filled with oil	15	1.4	32×16	0.08	—	—
Magnetic focusing	24	Human chest	2.18	36	—	30–36	—	—
Sensitive line	39	Human head	4.26	55	128×128	2.5	—	—

has proved highly instructive. Assuming the final signal-to-noise ratio in all the experiments to be about the same, this author compares the real time expenditures T in obtaining an image, taking into account, in contrast to Ref. 59, all the fundamental technical aspects, including the time for rotation and translation of the specimen, computer calculations, etc. Moreover, he attempts to reduce all the data to a single scale by recalculating them for two sets of standard conditions: a) $\nu_0 = 10$ MHz; diameter of specimen $d = 10$ cm; number of image elements $n^2 = 64 \times 64$, thickness of layer $h = 0.5$ cm; b) 5 MHz; 40 cm; 64×64; 2 cm, respectively.

Some results of this analysis, supplemented by newer data, are given in Table I.

We see from the table that the methods of the sensitive line and of selective excitation of a plane yield the greatest speed. Here, as we have noted, the former is considerably simpler to realize for large objects. These conclusions flatly contradict the theoretical estimates of the sensitivity according to Brunner and Ernst[59] that were discussed above. The discrepancy between the theoretical conclusions and their realization in experiments evidently indicates the imperfection of the contemporary apparatus. In future as technology progresses, we should expect a radical shortening of the time expenditures as compared with the data of the table. The time is approaching[49] when the image of a cross-section of the human body of quality not inferior to a television image, should take only about a second.

b) Instrumentation

The basis of an NMR introscope is the nuclear magnetic resonance spectrometer. In most of the methods this is a coherent pulsed Fourier spectrometer supplemented with gradient coils and automatic apparatus for scanning and recording the image on a display.

The construction of the gradient coils involves no fundamental difficulties; analogous devices have long been applied in studying diffusion with NMR (see, e.g., Ref. 9). Usually, in order to create the field gradient along the z axis (i.e., in the direction of $\mathbf{B}_0$), one employs two coaxial coils connected to oppose one another (see Fig. 7), while the gradients G_x and G_y are created by a system of linear, current-bearing conductors lying along the field $\mathbf{B}_0$.[29]

Thus, since we possess a firm basis in the development and manufacture of standard NMR Fourier spectrometers, it is relatively simple to proceed to making NMR introscopes. This has recently been done by the well-known "Brucker" company (West Germany), which in practically one year since the first successful demonstration of the biomedical potentialities of NMR introscopy, has begun to offer several types of introscopes that differ in the size of the working region and which allow one to study objects from several cm to the dimensions of the human body.

In addition, the instrumentation for NMR introscopy has a number of characteristic features dictated mainly by its biological and medical applications.

First of all, the dimensions of the specimen to be studied, which in routine NMR experiments usually do not exceed several mm, now can be as great as tens of centimeters (small experimental animals) or even a half-meter (cross-section of the human body). To enable the rf field to penetrate such objects without losing its homogeneity, one must choose a low enough working frequency: from 10–20 MHz in the first of the cited examples to about 1 MHz in the second one. This sharply contrasts with the tendency toward the maximal possible increase in ν in ordinary NMR spectroscopy, which is necessary to enhance the sensitivity and resolving power in terms of chemical shifts (see, e.g., Ref. 10). For comparison, we recall that the working frequency of modern commercial NMR spectrometers is as much as hundreds of MHz.

Naturally, the large volume of the specimen requires a special design of the magnet that produces the main field B_0. With account taken of the values of ν given above, for protons this field must amount to from 0.5 T for an aperture of the order of 10 cm to 0.03–0.1 T with a diameter of the object about 50 cm. While standard iron-core magnets are still applicable in the former case, in the latter case one must employ air-core solenoids (Fig. 15). Here the coils can be either ordinary[38-40] or superconductive.[22,26]

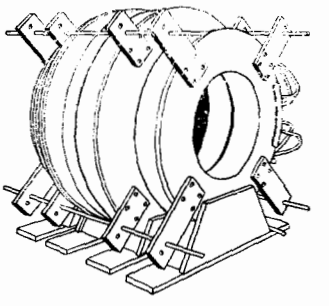

FIG. 15. Solenoid for obtaining NMR images of cross-sections of the human body.[38]

At first glance, the requirements on the homogeneity of the main magnetic field (and on constancy of its gradients) do not seem too severe: one can easily calculate that one must maintain the given field configuration with an accuracy of only about 10^{-5} to attain a resolution of 0.5 mm for $B_0 \approx 0.1$ T and $|\operatorname{grad} B_0| \approx 10^{-2}$ T/m. This value does not seem too frightful if we compare it with the relative homogeneity of magnetic fields of 10^{-8}–10^{-9} attained in the instruments for ordinary high-resolution NMR. Nevertheless, if we take account of the large volume of the working zone of the magnet, a certain effort is needed to satisfy the stated requirements. Further increase in the constancy and linearity of the field gradients being produced would open up a real prospect for chemical analysis *in vivo* by using high-resolution NMR spectra taken in an introscopic regime (see below, Sec. 4 c).

We should also note the high requirements imposed on the long-term stability of the magnetic field, which arises from the prolonged period for accumulation of signals during the construction of NMR images. Just as in ordinary NMR spectrometers, this problem is solved by automatic stabilization of the field with a reference NMR signal.

The large volume of the specimen also requires a special design of the receiving and transmitting high-frequency coils. We refer readers interested in this problem to Refs. 39, 40, 52, 60, and 65.

Finally we shall point out that the entire process of obtaining an image, including the application of the defined pulse sequences, the control of the magnetic field gradients, the scanning of the "sensitive" region, and the accumulation and interpretation of the output signals, etc., must be controlled by a fast on line computer (see, e.g., Refs. 40, 44). Such automation, which is generally characteristic of modern experimental technique, acquires special significance in this case, since this is essentially the only way to reduce the expenditure of time to a practically acceptable level.

c) Applications and prospects

Currently the application of NMR introscopy in biology and medicine is exciting the greatest interest. Along this line, the problem naturally arises of comparing the new method with the more traditional methods, mainly with x-ray reconstructive tomography,[1,66] which also yields images of thin layers (sections) of the object being studied.

The most evident advantage of NMR introscopy, which has been pointed out by most of the investigators, is the absence of radiations harmful to the organism. Apparently this eliminates the restrictions characteristic of the x-ray methods on the exposure time, number of projections, etc. Yet we should stress that the biological effect of ac and dc magnetic fields has as yet been studied insufficiently. However, the first data seem to indicate their safety to the patient.[39,67,68]

It is no less important that the nature of the contrast in NMR images fundamentally differs from all other introscopic methods. The possibility of obtaining a "chemical map" of the patient in any chosen cross-section is a unique, and perhaps the most attractive feature of NMR introscopy for medicine.

At the same time, the insufficiently high sensitivity of the method (see Sec. 4 a) leads to relatively long exposures. This involves prolonged immobilization of the patient, impairment of the sharpness of imaging of pulsing organs, etc. In this regard, introscopic practice as yet employs only the NMR signals from the most abundant nuclei having the maximal values of the factor γ—primarily protons ^{1}H. The high content of hydrogen in organic materials determines the immediate prospects of applications of NMR introscopy.

A powerful push in this direction has been given by the above-cited discovery of Damadian.[25] He established that the spin-lattice relaxation time τ_1 of protons in malignantly altered tissues is about twice as long as in normal tissues (0.2–0.4 s, as compared with 0.1–0.2 s, respectively). We have already noted that contrast involving the times τ_1 arises when the appropriate method is chosen in NMR imaging. For greater perspicuity, it is often emphasized by coloring the NMR tomogram in false colors coding the values of τ_1. A series of such images demonstrating the development of a malignant tumor in an experimental animal was at one time reprinted on the cover of the journal *Priroda*.[42] Another example was given in Ref. 24, which showed a transverse section of the chest of a patient—a 42-year-old woman—at the level of the third rib. The diagnosis was adenocarcinoma of the breast with metastasis to the right lung. The malignant tumor is visible as a light-blue strip that divides the cavity of the lung in two parts. The image was obtained by the method of magnetic focusing, and the exposure time was 36 min.

We must note that the reliability of diagnosis of cancer based on measuring τ_1 is apparently yet far from 100% (a detailed discussion of this problem is contained in the review[69]). Nevertheless, in the opinion of the specialists, this method can already be useful, e.g., in prophylactic examinations.[69] Work is also being carried out to increase its reliability by simultaneously monitoring the values of τ_1 and τ_2.[70]

In addition to malignant tumors, the objects of study of NMR introscopy can be edema (we recall that the amplitude of the NMR signal is highly sensitive to the water content) as well as other pathological changes. There is no space here to discuss all the possible applications of this method for diagnostic purposes, nor can one do this at present with enough assurance. Intensive searches and studies are needed (and are already being conducted) along this line.[67,68,71,72]

Special interest has been shown recently in NMR imaging of the brain,[39,40,67,68,73,74] which has been made possible by the development of NMR introscopes with a working aperture of about 55 cm.[40] Figure 16 shows one of the newest results.[68] The depicted layer about 1 cm thick was singled out by the sensitive-plane method by using a magnetic-field gradient oscillating in time (see Sec. 3 d and Fig. 7). The tomogram of this layer was constructed by the method of reconstruction

FIG. 16. NMR tomogram of a sagittal section of the head of a patient.[68] The arrow indicates the pathological structure—a thrombus-filled aneurysm in the intracranial segment of the carotid artery (see text). The image was obtained in 2 min from 128 projections. The working plane was singled out by the method of Hinshaw.[7]

FIG. 17. NMR tomogram of a cross-section of the head of a patient.[68] The plane of the section passes through the eyeballs, the bridge of the nose, and the conchae of the ears. The light spot indicated by the arrow is a tumor in the cerebello-pontine region.

from projections by Fourier transformation of the FI signal (Sec. 3a). The static gradient of the field B_0 was produced in the plane of the cross-section being imaged and had a magnitude of 60 μT/cm. The rotations of the gradient were carried out electrically without any mechanical displacements at all of the coils or of the patient. They employed 128 orientations of the gradient (projections). The main field amounted to 0.1 T, the NMR frequency was 4.26 MHz, the number of elements was 128×128, and the exposure time was about 2 min. The patient was a 59-year old woman in whom a pathological dilatation (aneurysm) had been found in the intracranial segment of the right carotid artery. The lightest regions in Fig. 16 correspond to the most intense NMR signals, which arise from the fat and muscle of the scalp. The bones of the skull and the dura mater, which contain practically no mobile protons, yield weak signals and look dark. The same pertains to the various cavities: the maxillary sinus and the frontal sinus, etc. The cerebral cortex looks like a diffuse light band, whereas the central light matter of the brain is rendered in various gradations of gray.

The blood in the vessels looks dark, since its movement in the inhomogeneous magnetic field averages and weakens the NMR signals. Therefore the lumen (cross-section) of the carotid artery has the form of a black spot. The clearly distinguished lighter structure around it constitutes the aneurysm, which is filled with a thrombus.[68]

Another NMR tomogram obtained[68] by the same method is shown in Fig. 17. The patient is a 36-year-old woman with the diagnosis of a tumor in the cerebello-pontine region near the brain stem. In the tomogram the tumor can be seen as a region of elevated brightness.

In Refs. 67 and 68 such NMR images of cross-sections of the brain are correlated in detail with the x-ray tomograms. They conclude that the NMR method yields valuable information on pathological changes in the brain, including tumors, and proves no more expensive than the x-ray method.

Another direction in the biomedical applications of NMR introscopy involves the sensitivity of the NMR signals to the velocity of a liquid flowing through diamagnetic tubes.[71,75] Model experiments have been reported[76] on obtaining transverse sections of the pulsating flow of a liquid inside a glass tube placed in a liquid of the same type, but at rest. The authors of this study deem possible similar experiments on the aorta and other large vessels of man, and even on small vessels when the methodology is perfected. The realization of this idea would make it possible to measure the "local pulse" at any point of the living organism.

NMR based on ^{19}F nuclei is practically not inferior in sensitivity to proton NMR, though the biomedical applications of ^{19}F imaging are far less promising because of the extremely small content of fluorine in the organism. However, this circumstance also can be utilized: harmless compounds of fluorine can be introduced into the patient or into an experimental animal as a contrast material, which one proposes to trace by NMR imaging. This idea has been advanced by the authors of Ref. 32, who have performed successful experiments on model objects. They also have pointed out the possible applications of this method for visualizing the flow of fluorine-containing blood substitutes.

As the sensitivity of the apparatus has been increased, NMR introscopy based on ^{31}P nuclei has acquired a serious significance. As we know, phosphorus-containing compounds (ATP and a number of others) play an extremely important role in the energetics and metabolism of living organisms. The sensitivity of ^{31}P NMR spectrometers is only an order of magnitude smaller than for protons, whereas the chemical shifts of the lines of ^{31}P are much larger, and are strongly distinguished for a number of the biologically important compounds of phosphorus. This situation allows us to rely on obtaining high-resolution ^{31}P spectra in an NMR introscopic regime, i.e., detailed chemical maps of metabolic processes in the organism being studied. It would be hard to overestimate the importance of this result—it suffices to point out the high

sensitivity of high-resolution ^{31}P spectra to the pathological changes in ischemia, myocardial infarction, etc.[69] Intensive work is being directed along this line.

The first successful experiments have been described in Refs. 77–79. Here the authors[78] have developed a special methodology that allows one to distinguish even relatively small chemical shifts.

NMR introscopy based on nuclei of low abundance (^{13}C, ^{17}O, etc.) has not been described, although ideas have been expressed on employing these isotopes as markers for special diagnostic purposes.[70,71]

Other applications of NMR introscopy have as yet been weakly developed, and they do not extend beyond preliminary ideas and proposals. Among them we can note the possible observation of biological processes in selected cross-sections of living plants in the course of vegetating; harmless radiography of seeds with local measurements of concentrations and characteristics of oils, proteins, and other substances, etc.

As we know, the "ordinary" broad-line NMR spectroscopy, as well as the measurement of nuclear relaxation times, are being successfully applied for quality control of margarine, butter, cheese, and other food products (see, e.g., Refs. 80, 81), and also for measuring the moisture content of various materials.[82] The combination of these methodologies with the technique of introscopy would enable nondestructive monitoring throughout the volume of a product in its commodity form. The topic can also arise of technical defectoscopy of nonmetallic (e.g., polymeric) wares. However, here the competition from the traditional methods will apparently be more successful than in biology and medicine.

Granted further progress in spatial resolution, NMR introscopy can prove useful in studying microscopic objects and structures, such as the cells of plants and animals, impurities and defects in crystals, etc. Here, apparently, the methods inspiring the greatest hopes are selective excitation (Secs. 3 e, f), and also a transfer of the ideas of NMR introscopy into electron paramagnetic resonance (EPR).[83,84] Thus, the spatial distribution of the nitrogen impurity in diamond crystals has been found by EPR introscopy,[83] and a spatial resolution of about 10 μm has been attained[84] in a model object.

The same methods can be used also in nuclear quadrupole resonance (NQR). In particular, the development of an NQR introscopic technique based on ^{14}N nuclei has been developed.[85] One can use it to detect the presence of nitrogen compounds at distances up to 80 cm from the high-frequency coil. The authors[85] proposed to use this for detecting explosives in closed volumes.

Undoubtedly, the list presented above of possible applications of the methods of NMR introscopy does not exhaust its possibilities. It will expand as the methodology and instrumentation are perfected.

5. CONCLUSION

The entire field of studies described in this review began to be revealed distinctly and to take shape in 1974–1975, while by 1980 the leading foreign instrument-making firms had developed and shipped to customers the first NMR-introscope units for biomedical applications. In the same year the first results of clinical trials began to be discussed in print.[67,68] Undoubtedly the very fact of such a vigorous progress of the new (and incidentally not at all cheap) method indicates its high prestige in the eyes of the specialists—developers and customers.

Of course, the development of NMR introscopy is not at all finished, while its future is yet not fully clear. The statements on its significance vary from the ecstatic proclamation of a "new era in medicine" (Damadian *et al.*[23]) to the restrained, and sometimes even skeptical attitude on the part of the professionally cautious practicing physicians. Apparently the truth lies somewhere between these extreme viewpoints. We must agree with one of the founders of x-ray reconstructive tomography, Nobel prize winner G. N. Hounsfield, who thinks that NMR introscopy will not so much compete with the other tomographic methods as essentially supplement them.[66]

In order to reveal fully the actual practical potentialities of NMR introscopy, we need first of all global biomedical and physiological studies. Along with this, we must work on the further improvement of the sensitivity, speed, and spatial resolution of NMR introscopes—perhaps by fundamentally new solutions. Finally, the problem is becoming timely of producing commercial instrumentation for NMR introscopy. In particular, the latter is associated with the increased production of pulsed NMR spectrometers, which are a necessary constituent part of the introscopes. Taking into account the high cost of such instruments (about 100 thousand rubles), we can address not only the scientific and technical problem, but also the problem of the national economy.

In closing, we should like to call the attention of the readers to the extreme fruitfulness of the magnetic-resonance methods, which stem from the famous discovery of E. K. Zavoiskii.[86] Repeatedly in the past decades, the skeptics have predicted the exhaustion of this field of science. However, each time it has turned to us a new, often unexpected facet and has given life to new and topical scientific approaches. For example, it suffices to recall the founding of solid-state quantum electronics,[87] the development of the methods of dynamic polarization of nuclei,[88] and the rise of high-resolution NMR in solids.[53] Now NMR introscopy arises in the same sequence, eloquently indicating that the potentialities of magnetic-resonance methods are yet far from exhaustion.

[1]R. Gordon, G. T. Herman, and S. A. Johnson, Scientific American 233, No. 4, 56 (1975).
[2]A. Abragam, The Principles of Nuclear Magnetism, Clarendon Fress, Oxford, 1961 (Russ. Transl., IL, M., 1963).

[3]A. Loesche, Nuclear Induction [Russ. Transl., IL, M., 1963].
[4]A. G. Lundin and É. I. Fedin, Yadernyĭ magnitnyĭ rezonans. Osnovy i primeneniya (Nuclear Magnetic Resonance. Foundations and Applications), Nauka, Novosibirsk, 1980.
[5]P. C. Lauterbur, Nature 242, 190 (1973).
[6]P. Mansfield and P. K. Grannell, J. Phys. C 6, L422 (1973).
[7]W. S. Hinshaw, Phys. Lett. A 48, 87 (1974).
[8]R. Damadian, L. Minkoff, M. Goldsmith, M. Stanford, and J. Koutcher, Science 194, 1430 (1976).
[9]T. Farrar and É. Bekker, NMR Pulsed and Fourier Spectroscopy [Russ. Transl., M., 1973].
[10]J. W. Emsley, J. Feeney, and L. H. Sutcliffe, High Resolution Nuclear Magnetic Resonance Spectroscopy, 1st edn., Pergamon, Oxford, 1965–1966 (Russ. Transl., Mir, M., 1968).
[11]R. Gordon and C. T. Herman, Comm. Assoc. Comput. Mach. 14, 759 (1971).
[12]P. C. Lauterbur, Pure and Appl. Chem. 40, 149 (1974).
[13]H. R. Brooker and W. S. Hinshaw, J. Magn. Reson. 30, 129 (1978).
[14]P. Lauterbur *et al.*, J. Am. Chem. Soc. 97, 6866 (1975).
[15]C.-M. Lai, J. Shook, and P. Lauterbur, Chem. Biomed. Envir. Instr. 9, 1 (1979).
[16]P. Bendel, C.-M. Lai, and P. Lauterbur, J. Magn. Reson. 38, 343 (1980).
[17]P. Lauterbur, Abstracts of Joint ISMAR-AMPERE Intern. Conference on Magnetic Resonance, Delft, The Netherlands, 1980, p. 56.
[18]A. Kumar, D. Welti, and R. R. Ernst, J. Magn. Reson. 18, 69 (1975); Naturwissenschaften 62, 34 (1975).
[19]R. Freeman and G. A. Morris, Bull. Magn. Reson. 1, 5 (1979).
[20]G.-J. Béné *et al.*, C. R. Acad. Sci. Ser. B 284, 141 (1977); B. Borcard *et al.*, *ibid.* 288, 41 (1979).
[21]G.-J. Béné, Phys. Rep. 58, 213 (1980).
[22]R. Damadian *et al.*, Naturwissenschaften 65, 250 (1978).
[23]R. Damadian, M. Goldsmith, and L. Minkoff, Physiol. Chem. Phys. 9, 97 (1977).
[24]R. Damadian, M. Goldsmith, and L. Minkoff, *ibid.* 10, 285 (1978).
[25]R. Damadian, Science 171, 1151 (1971).
[26]L. Minkoff *et al.*, Physiol. Chem. Phys. 9, 101 (1977).
[27]M. Goldsmith *et al.*, *ibid.* 9, 105 (1977).
[28]W. S. Hinshaw, in: Proc. 18th AMPERE Congress, Nottingham, 1974, eds. P. S. Allen, E. R. Andrew, and C. A. Bates, North-Holland, Amsterdam, 1975, Vol. 2, p. 433.
[29]W. S. Hinshaw, J. Appl. Phys. 47, 3709 (1976).
[30]E. R. Andrew, Phys. Bull. 28, 323 (1977).
[31]W. S. Hinshaw, P. A. Bottomley, and G. N. Holland, Nature 270, 722 (1977).
[32]G. N. Holland, P. A. Bottomley, and W. S. Hinshaw, J. Magn. Reson. 28, 133 (1977).
[33]P. A. Bottomley *et al.*, Phys. Med. Biol. 22, 71 (1977).
[34]W. S. Hinshaw *et al.*, Brit. J. Radiol. 51, 273 (1978).
[35]W. S. Hinshaw *et al.*, Neuroradiology 16, 607 (1978).
[36]P. A. Bottomley, Cancer Res. 39, 468 (1979).
[37]E. R. Andrew *et al.*, in: Magnetic Resonance and Related Phenomena; Proc. 20th AMPERE Congress, Tallinn, 1978, eds. E. Kundla, E. Lippmaa, and T. Saluvere, Springer-Verlag, Berlin, 1979, p. 53.
[38]E. R. Andrew, Philos. Trans. R. Soc. London Ser. B 289, 471 (1980).
[39]W. Holland, W. Moore, and R. Hawkes, J. Comp. Assist. Tomography 4, 1 (1980); Brit. J. Radiol. 53, 253 (1980).
[40]W. Moore and G. Holland, Philos. Trans. R. Soc. London Ser. B 289, 133 (1980).
[41]F. T. Meiere and F. C. Thatcher, J. Appl. Phys. 50, 4491 (1979).
[42]É. I. Fedin, Priroda 1980, No. 4, 77.
[43]A. N. Garroway, P. K. Grannell, and P. Mansfield, J. Phys. C 7, L457 (1974).
[44]P. Mansfield, A. A. Maudsley, and T. Baines, *ibid.*, Ser. E 9, 271 (1976).
[45]P. Mansfield and A. A. Maudsley, *ibid.*, Ser. C 9, 1409 (1976).
[46]P. Mansfield and A. A. Maudsley, J. Magn. Reson. 27, 101 (1977).
[47]P. Mansfield and A. A. Maudsley, Brit. J. Radiol. 50, 188 (1977).
[48]P. Mansfield and I. L. Pykett, J. Magn. Reson. 29, 355 (1978).
[49]Mansfield *et al.*, *ibid.*, 33, 261 (1979).
[50]P. Mansfield, I. Pykett, P. Morris, and R. Coupland, Brit. J. Radiol. 51, 921 (1978).
[51]P. Mansfield and P. K. Grannell, Phys. Rev. B 12, 3618 (1975).
[52]D. I. Hoult, J. Magn. Reson. 33, 183 (1979); 38, 369 (1980).
[53]U. Häberlen and M. Mering, High-Resolution NMR in Solids [Russ. Transl., Mir, M., 1980].
[54]R. A. Wind and C. S. Yannoni, J. Magn. Reson. 36, 269 (1979).
[55]C. S. Yannoni and H.-M. Vieth, Phys. Rev. Lett. 37, 1230 (1976).
[56]M. Lee and W. I. Goldburh, Phys. Rev. A 140, 1261 (1965).
[57]A. E. Mefed and V. A. Atsarkin, Zh. Eksp. Teor. Fiz. 74, 720 (1978) [Sov. Phys. JETP 47, 378 (1978)].
[58]V. A. Atsarkin, A. E. Mefed, and M. I. Rodak, Fiz. Tverd. Tela (Leningrad) 21, 2672 (1979) [Sov. Phys. Solid State 21, 1537 (1979)].
[59]P. Brunner and R. Ernst, J. Magn. Reson. 33, 83 (1979).
[60]D. I. Hoult and P. C. Lauterbur, *ibid.*, 34, 425 (1979).
[61]P. A. Bottomley and E. R. Andrew, Phys. Med. Biol. 23, 630 (1978).
[62]J. M. Libove and J. R. Singer, J. Phys. E 13, 38 (1980).
[63]P. A. Bottomley, J. Magn. Reson. 36, 121 (1979).
[64]I. L. Pykett and P. Mansfield, Phys. Med. Biol. 23, 961 (1978).
[65]T. Baines and P. Mansfield, J. Phys. E 9, 809 (1976).
[66]G. N. Hounsfield, Science 210, 22 (1980).
[67]W. Moore, G. Holland, and L. Kreel, CT: Comp. Tomography 4, 1 (1980).
[68]R. Hawkes, G. Holland, W. Moore, and B. Worthington, J. Comp. Assist. Tomography 4, 577 (1980).
[69]D. P. Hollis, Bull. Magn. Reson. 1, 27 (1979).
[70]J. Koutchar, M. Goldsmith, and R. Damadian, Cancer 41, 174 (1978).
[71]C. M. Lai, W. House, and P. Lauterbur, Nuclear Magnetic Resonance Zeugmatography for Medical Imaging: Preprint of State University of New York at Stony Brook, 1980.
[72]J. Mallard, J. Hutchison, W. Edelstain, *et al.*, Philos. Trans. R. Soc. London Ser. B 289, 519 (1980).
[73]G. N. Holland, R. C. Hawkes, and W. S. Moore, J. Comp. Assist. Tomography 4, 429 (1980).
[74]G. De Chiro, *ibid.*, p. 210.
[75]A. Garroway, J. Phys. D 7, L159 (1974).
[76]P. Lauterbur and C. M. Lai, in: Proc. of 1977 Devices and Techn. Branch Contractors Conference Program, Government Printing Office, Washington, 1978.
[77]P. Bendel, C. M. Lai, and P. Lauterbur, J. Magn. Reson. 38, 343 (1980).
[78]S. J. Cox and P. Styles, *ibid.*, 40, 209 (1980).
[79]P. Bottomley and R. Nunnally, see Ref. 17, p. 21.
[80]P. Mansfield and C. Horn, J. Food Techn. 7, 53 (1972).
[81]A. F. Babkin *et al.*, Pishchevaya Tekhnologiya 1976, No. 6, 130.
[82]S. P. Gabuda, Yadernyĭ magnitnyĭ rezonans v kristallogidratakh i gidratirovannykh belkakh (Nuclear Magnetic Resonance in Crystal Hydrates and Hydrated Proteins), Nauka, Novosibirsk, 1978.
[83]M. Hoch and A. Day, Solid State Commun. 30, 211 (1979).
[84]W. Karthe and E. Wehrsdorfer, J. Magn. Reson. 33, 107

(1979).
[85]T. Hirschfeld and S. M. Klainer, J. Mol. Struct. 58, 63 (1980).
[86]E. K. Zavoĭskiĭ, Doctoral dissertation, Institute of Physics of the Academy of Sciences of the USSR, 1944; J. Phys. USSR 9, 245 (1945).
[87]J. R. Singer, Masers, Wiley, New York, 1959 (Russ. Transl., IL, M., 1961).
[88]C. D. Jeffries, Dynamic Nuclear Orientation, Interscience, New York, 1963 (Russ. Transl., Mir, M., 1965).
[89]L. G. Dubitskiĭ, Defektoskopiya 1971, No. 6, 53.

Translated by M. V. King